The Seventh International Colloquium on Bluff Body Aerodynamics and Applications (BBAA7)
Shanghai, China; September 2-6, 2012

Discussion of design wind force coefficients for hyperbolic paraboloid free roofs

Fumiyoshi Takeda [a], Tatsuya Yoshino [b], Yasushi Uematsu [c]

[a] *Structural Engineer, Technical Research Center, R&D Division, Taiyo Kogyo Corporation, 3-20, Syodai-Tajika, Hirakatashi, Osaka, Japan*
[b] *Researcher, Technical Research Center, R&D Division, Taiyo Kogyo Corporation, 3-20, Syodai-Tajika, Hirakatashi, Osaka, Japan*
[c] *Professor, Department of Architecture and Building Science, Tohoku University, Sendai, Japan*

ABSTRACT: The present paper discusses the design wind force coefficients for hyperbolic paraboloid (hereafter "HP") free roofs constructed of membrane structures, based on a structural analysis for various conditions as well as on a CFD analysis. The application of the wind force coefficients obtained from wind tunnel experiments with rigid models is investigated. The influences of roof deformation on the wind forces and the resultant load effects are also investigated.

KEYWORDS: Wind force coefficient, Hyperbolic paraboloid roof, Membrane structure, Wind tunnel experiment, CFD (Computational Fluid Dynamics), Structural analysis.

1 INTRODUCTION

The purpose of the present study is to propose the design wind force coefficients providing the equivalent static wind loads on HP-shaped membrane structures, in which the dynamic load effect is considered appropriately. Pun and Letchford (1993) reported the analysis of an HP-shaped tension membrane roof subjected to fluctuating wind loads (Ref. 1). To the authors' best knowledge, few studies of wind loads on HP-shaped membrane free roofs have been done since. Even for free roofs of the other shapes, the number of studies on the wind loads is quite limited. Recently, Nagai et al. (2012) (Ref. 2) have investigated the wind loads on a horn-shaped membrane structure.

The authors have carried out a series of wind tunnel experiments and CFD analyses to investigate the wind forces on rigid free roofs with various configurations, i.e. gable, troughed, mono-sloped, and HP-shaped roofs (Ref. 3, 4). Figure 1(a) shows an HP-shaped rigid model used in the wind tunnel experiments. Based on the results, we have proposed the design wind force coefficients for HP free roofs (Ref. 5), assuming that the roof is supported by the four corner columns (see Fig. 1(b)), in which the axial forces involved in the columns are regarded as the

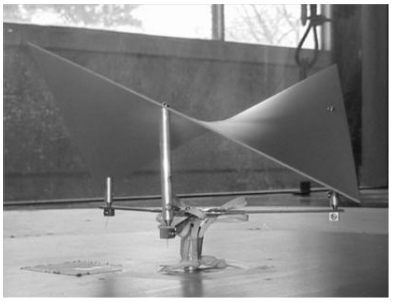

(a) Picture of an HP model

(b) Four corner columns

Figure 1. Experimental model and a supporting system

most important load effect for discussing the design wind force coefficients.

In practice, however, there are many other supporting systems, such as a 'post and guy cable system'. Moreover, the membrane roof is not rigid but rather flexible, the deformation of which is larger than that of conventional roofs such as metal roofs. Therefore, regarding the application of the proposed wind force coefficients, the following questions have arisen: (i) Can they be applied to membrane structures with the other supporting systems? The structural characteristics such as arrangement and stiffness of the members may affect the responses significantly (Ref. 6); (ii) Can they be applied to flexible roofs that deform under wind loading? The roof deformation may change the wind force significantly; (iii) Do they overestimate or underestimate the wind loads for suspension structures?

Therefore, the present paper investigates these subjects, based on structural analyses of the roofs with three types of structural systems and CFD analyses of the wind forces on the deformed roof. Finally, a discussion is made of the design wind force coefficients.

2 DEFINITION OF WIND FORCE AND MOMENT COEFFICIENTS

2.1 *Roof types*

Three models (Models A - C) with different rise/span (or sag/span) ratios have investigated in previous studies (Fig. 2). Focus is on the model A in the present study. The plan of the roof is a square of 15 m by 15 m, and the mean roof height H is 8 m in full scale.

2.2 *Definitions*

Figure 3 shows the definition of the aerodynamic forces and moments, where D and L represent the drag and lift, respectively; M_x and M_y are the moments about the x and y axes, respectively. These values are normalized as follows:

$$C_D = \frac{D}{q_H ha} \quad C_L = \frac{L}{q_H S} \quad C_{Mx} = \frac{M_x}{q_H Sa} \quad C_{My} = \frac{M_y}{q_H Sa} \qquad (1), (2), (3), (4)$$

where q_H = reference velocity pressure at the mean roof height; h = difference in height for the roof ; a = horizontal (projection) width of the roof; and S = projection area of the roof. For the purpose of simplicity, the design wind force coefficients on the roof are specified by two uniformly distributed values (C_{NW} and C_{NL}) over the windward and leeward halves (Fig. 4), which are defined by

$$C_{NW} = \frac{N_W}{q_H S/2} \quad C_{NL} = \frac{N_L}{q_H S/2} \qquad (5), (6)$$

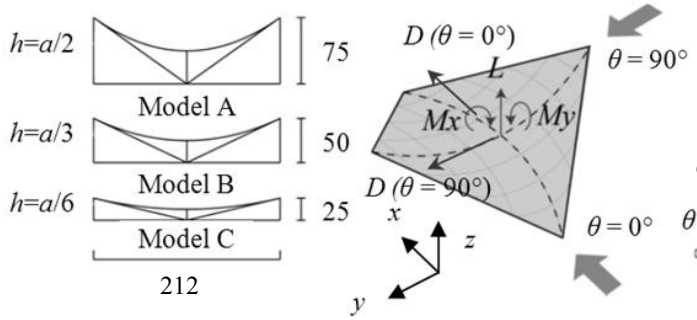

Figure 2. Roof shapes (mm)

Figure 3. Definition of D, L, M_x and M_y

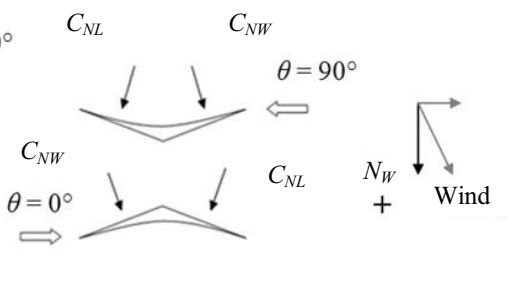

Figure 4. Dimensions of C_{NL} and C_{NW}

where N_W and N_L represent the normal wind forces, positive downward, on the windward and leeward halves, respectively. The coefficients C_{NW} and C_{NL} can be represented by C_L and C_{My} for the wind direction $\theta = 0°$ as follows:

$$C_{NW} = -C_L - 3\sqrt{2}C_{My} \quad C_{NL} = -C_L + 3\sqrt{2}C_{My} \qquad (7), (8)$$

3 WIND TUNNEL EXPERIMNET

3.1 *Arrangement and Procedure*

The wind tunnel model is made of 1 mm thick acrylic plate with a geometric scale of 1/100. Figure 1(a) shows a model mounted on the force balance that was designed, built and gauged for this experiment. The Y-shaped force balance is made of 1.2 mm thick phosphor bronze in order to measure the lift L and the aerodynamic moments M_x and M_y (Ref. 5). The experiments were carried out in a boundary layer wind tunnel with a working section 1.4 m wide, 1.0 m high and 6.5 m long at the Department of Architecture and Building Science, Tohoku University, Japan. A turbulent boundary layer with a power law exponent of α = 0.18 for the mean velocity profile was generated on the wind tunnel floor. The turbulence intensity I_u and longitudinal length scale L_x of the flow at a height of z = 100 mm are 0.17 and 0.16 m, respectively. The measurements were carried out at a wind speed of $U_H \approx 6$ m/s at the mean roof height H. The design wind speed is assumed 31.5 m/s, as a typical value of strong wind events; therefore, the velocity scale is approximately 1/5.25. The geometric scale of the model and the velocity scale yield a time scale of approximately 1/19. The wind direction θ is changed from 0° to 90° at a step of 15°. The outputs of the strain meters were sampled simultaneously at a rate of 200 Hz for a period of 32 sec, which approximately corresponds to 10 min in full scale. The measurements were repeated six times under the same condition. The statistics of the aerodynamic coefficients are evaluated by applying ensemble average to the results of the six consequence runs. Figure 5 shows a phase-plane representation of the C_L - C_{My} relation when θ = 0°. The circle in the figure represents a condition where the C_L value becomes an extreme (the maximum and minimum peak) in each run. It is seen that the peak values of C_L and C_{My} do not necessarily occur at the same time. The envelope of the trajectory is approximated by a hexagon as shown in Figure 6.

4 PROPOSED DESIGN WIND FORCE COEFFICIENTS

4.1 *Design wind force coefficients*

The authors have proposed a procedure to obtain the design wind force coefficients (Ref. 5),

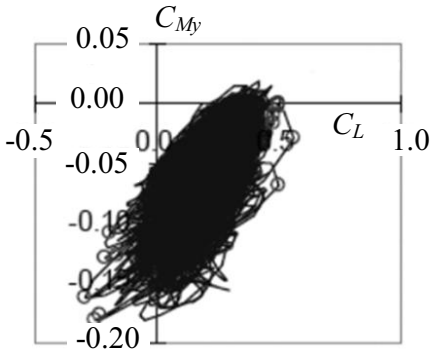

Figure 5. C_L- C_{My} trajectory for Model B (h/a = 1/3)

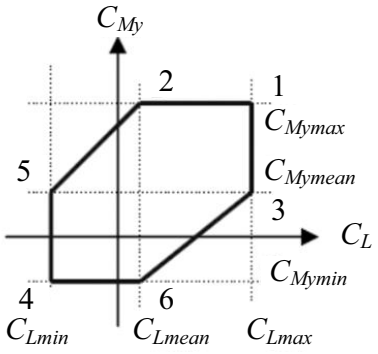

Figure 6. Model of the envelope of C_L-C_{My} trajectory

Table 1. Basic values of the wind force coefficients

Apex	Combination of C_L and C_{My}/C_{Mx} *1)	Wind direction $\theta = 0°$		Wind direction $\theta = 90°$	
		C_{NW0}	C_{NL0}	C_{NW0}	C_{NL0}
1	$C_{Lmax} + C_{Mymax}/C_{Mxmax}$	-0.65	-0.72	-0.37	0.11
2	$C_{Lmean} + C_{Mymax}/C_{Mxmax}$	-0.31	-0.38	0.02	0.50
3	$C_{Lmax} + C_{Mymean}/C_{Mxmean}$	-0.40	-0.97	-0.89	0.63
4	$C_{Lmin} + C_{Mymin}/C_{Mxmin}$	0.80	-0.67	-0.56	2.31
5	$C_{Lmin} + C_{Mymean}/C_{Mxmean}$	0.35	-0.22	0.12	1.63
6	$C_{Lmean} + C_{Mymin}/C_{Mxmin}$	0.39	-1.08	-1.17	1.70

*1) Using C_{My} for $\theta = 0°$, C_{Mx} for $\theta = 90°$

assuming that the roof is rigid and simply supported by the four corner columns. The procedure is summarized as follows. Focus is on the incremental axial forces induced in the columns by the wind forces as one of the most important load effects for evaluating the wind force coefficients. The incremental axial forces are computed for the combination of C_L and C_{My} (for $\theta = 0°$) or C_{Mx} (for $\theta = 90°$) at each apex of the hexagon as shown in Figure 6. The roof is divided into two areas, i.e. the windward and leeward halves, and the design wind force coefficient is assumed constant in each area. The design wind force coefficients C^*_{NW} and C^*_{NL} for these halves are presented as follows:

$$C^*_{NW} = \frac{\gamma C_{NW0}}{G_f} \qquad C^*_{NL} = \frac{\gamma C_{NL0}}{G_f} \tag{9), (10}$$

where C_{NW0} and C_{NL0} are the basic values, computed from Equations (7) and (8), respectively, by using a combination of C_L and C_{My} (or C_{Mx}) at each apex of the hexagon. Table 1 summarizes the values of C_{NW0} and C_{NL0} at the six apexes for two wind directions, i.e. $\theta = 0°$ and $\theta = 90°$ (see Fig. 4). In the study, two sets of the C_{NW0} and C_{NL0} values are selected from the six sets at the apexes, which induce the maximum tension and compression in the columns.

The value of γ in Equations (9) and (10) is a correction factor for the influence of wind direction (Ref. 5). It is obtained by calculating the ratio of the actual maximum or minimum axial force in a wind direction range of 0° ± 45° (WD1) or 90° ± 45° (WD2) to the predicted value from C_{NW0} and C_{NL0}. In practice, the value of $\gamma = 1.0$ is used in the present study, because the maximum tension and compression are induced when $\theta = 0°$ for WD1 and $\theta = 90°$ for WD2. Note that this is not the case for gable and troughed roofs (Ref.3). G_f is the gust effect factor for considering the dynamic load effect. The value of $G_f = 2.0$ is used for evaluating the design wind force coefficients in this study.

5 EFFECT OF ROOF SUPPORTING SYSTEM

5.1 *Analytical models*

Three structural systems are often used for membrane structures, i.e. frame, suspension and air-supported types. Focus is on the frame and suspension types in the present analyses. Figure 7 shows the analytical models. In Frame-model 1 (F1 model), the roof structure is constructed of the perimeter girders and binding beams, which divide the roof area into twelve zones (Fig. 7(a)). The frame is covered with pre-stressed membrane. The pre-stress is 4 kN/m both in the warp and fill (weft) directions of membrane. The warp direction is shown in Figure 7(b). The fill direction is perpendicular to the warp direction. The self-weight of membrane is assumed 12 N/m^2. Frame-model 2 (F2 model) consists of the perimeter girders and pre-stressed membrane (Fig. 7(b)). In

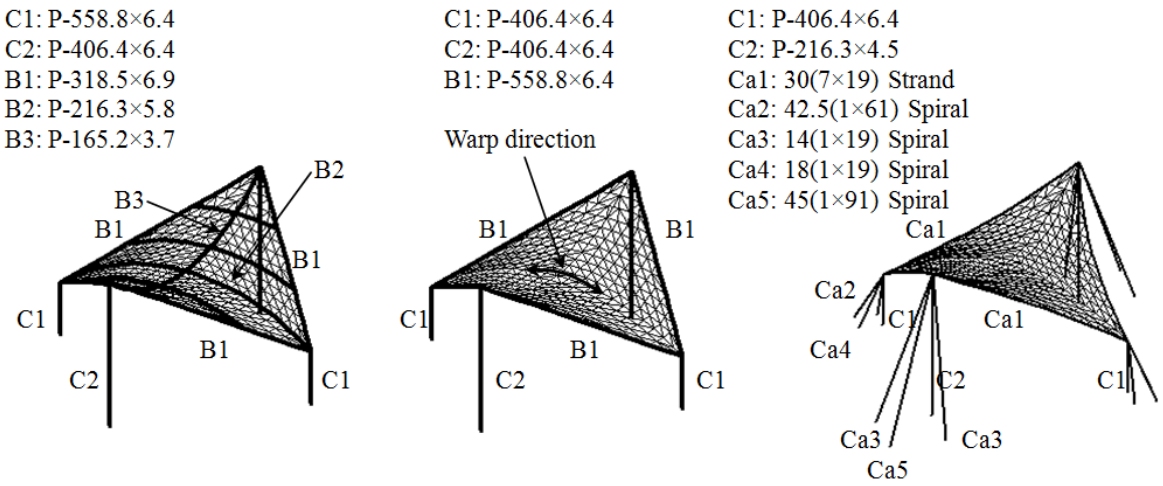

(a) Frame-model 1 (F1) (b) Frame-model 2 (F2) (c) Suspension-model (S1)

Figure 7. Analytical models

Table 2(a). Membrane (t: Thickness)

Tensional stiffness:	$E_w \times t$ = 1284.67 kN/m (Warp)
	$E_f \times t$ = 861.024 kN/m (Fill)
Poisson's ratio:	v_w = 0.85 (Warp) v_f = 0. 57 (Fill)
Shear modulus:	$G \times t$ = 56.9766 kN/m

Table 2(b). Cable

Elastic modulus:	$E = 1.37 \times 10^8$ kN/m^2 (Strand)
	$E = 1.57 \times 10^8$ kN/m^2 (Spiral)

Table 2(c). Beam and Post

Elastic modulus:	$E = 2.05 \times 10^8$ kN/m^2
Poisson's ratio:	$v = 0.3$

these Frame-models, the roof girders are supported by the four corner columns. On the other hand, Suspension-model (S1 model) consists of the curved perimeter cables and pre-stressed membrane; the roof is supported by the posts and guy cables at the four corners, as shown in Figure 7(c). The column bases of the F1 and F2 models are fixed, while the posts of the S1 model are pin-supported. The connection of elements in the F1 and F2 models is rigid. The material of the columns, beams, posts and cables is steel; that of the membranes is PTFE-coated glass fiber plain-weave fabric. The projection area of the S1 model is approximately 82% of that of the Frame models because of the curved perimeters. The S1 model is the most flexible among these three models, which causes the largest deformation to the roof under wind loading. On the other hand, the F1 model is relatively rigid. Moreover, the roof membrane slightly deforms in the downward direction due to the self-weight. Therefore, the initial shapes of these three roofs are slightly different from each other due to the difference in the supporting system.

5.2 *Structural analyses*

The structural analyses are conducted by using a program named MAGESTIC, in-house software of Taiyo Kogyo Corp., based on a finite element method with the Newton-Raphson method, in which the geometrical nonlinearity is taken into account. The membrane material is assumed orthotropic and elastic. Furthermore, it is assumed that the membrane carry only tension; in other words, it does not resist compression and bending moment. The design wind speed is 31.5 m/s. The corresponding velocity pressure is 605 N/m^2. The six wind force coefficients calculated from the C_{NW0} and C_{NL0} values in Table 1 for each wind direction are used in order to find the critical condition that gives the maximum load effect; they are provided by the combination of C_L and C_{My} (or C_{Mx}) corresponding to the six apexes of the hexagon. In the analyses, the stresses

are calculated based on the Building Standard Law of Japan and Design Standard for Steel Structures published by the Architectural Institute of Japan. For the membranes and cables, tensile stresses are calculated from the tensile forces; for the beams and columns, the extreme fiber stresses are calculated by combining the axial forces and bending moments; for the posts of the S1 model, axial stresses are calculated from the axial forces. The allowable stresses and

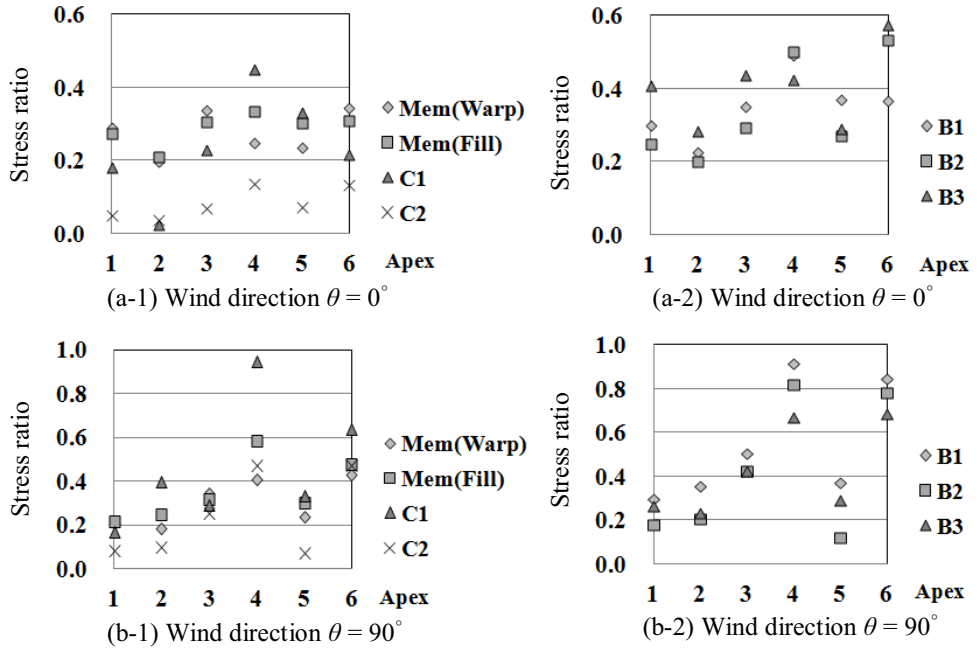

(a-1) Wind direction $\theta = 0^{\circ}$ (a-2) Wind direction $\theta = 0^{\circ}$

(b-1) Wind direction $\theta = 90^{\circ}$ (b-2) Wind direction $\theta = 90^{\circ}$

Figure 8. Stress ratio for Frame-model 1 (F1)

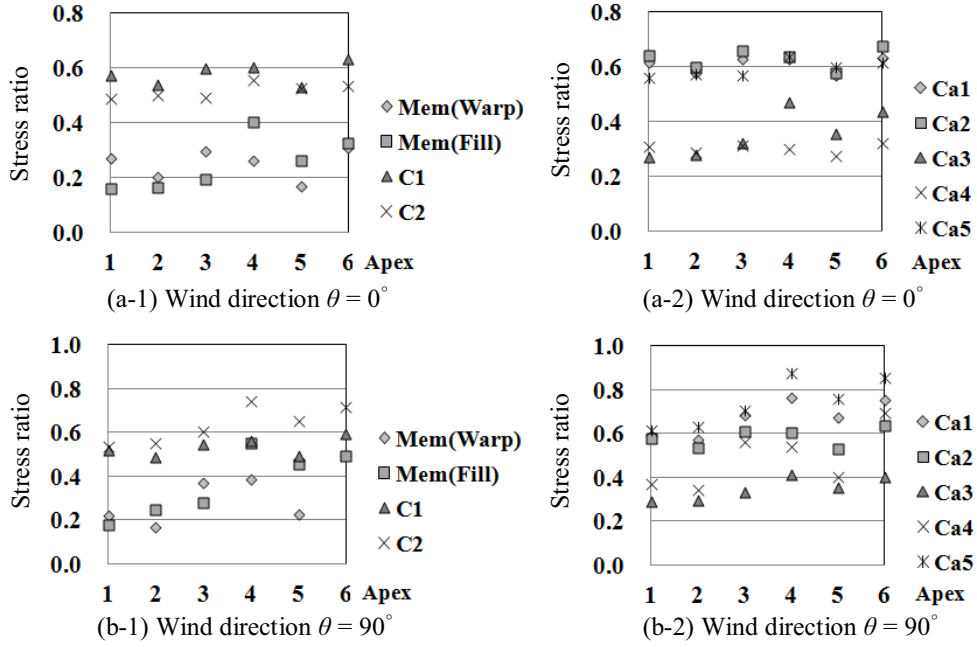

(a-1) Wind direction $\theta = 0^{\circ}$ (a-2) Wind direction $\theta = 0^{\circ}$

(b-1) Wind direction $\theta = 90^{\circ}$ (b-2) Wind direction $\theta = 90^{\circ}$

Figure 9. Stress ratio for Suspension model (S1)

Table 3. Load combination providing the maximum stress

Model	Wind direction	Member	Maximum Apex	Expected Apex	Ratio
F1	0°	Mem (Warp)	6	3	1.38
		B2	6	4	1.06
		B3	6	3	1.36
F2	0°	Mem (Warp)	6	3	1.01
		B1	6	4	1.03
S1	0°	Mem (Warp)	6	3	1.18
		C1	6	4	1.05
		Ca1	6	4	1.01
		Ca2	6	3	1.06
		Ca4	6	3	1.07

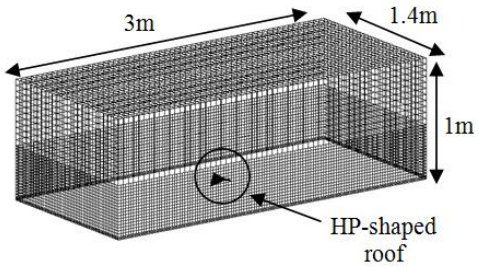

Figure 10. Numerical model

material constants (Table. 2) are also determined based on the Law and Standard. Moreover, the ratio of the computed stress to the allowable stress is calculated, which is called 'stress ratio' in the present paper. The each member size is determined so that the stress ratios are less than 1.0. Figure 8 and 9 shows the results of structural analyses for the F1 and S1 model, respectively. In the figures, the maximum stress ratios for the members, i.e. membrane (Mem), cable, column, beam and post, are shown for the six apexes of the hexagon in Figure 6.

5.3 *Load effects*

The design wind force coefficients are provided by the two combinations of C_L and C_{My} (or C_{Mx}) so that the incremental axial force induced in the columns becomes the maximum compression and tension. In this HP-shaped roof case, the two combinations are the ones corresponding to Apexes 3 and 4 for the wind direction $\theta = 0^o$ and Apexes 4 and 6 for the wind direction $\theta = 90^o$. The combination corresponding to one of the two Apexes (hereafter called "expected Apex") is expected to become the critical condition for the stress ratio of the members.

In Figures 8 and 9, the results for the wind direction $\theta = 90^o$ indicate that the stress ratio of them becomes the maximum for the combination of C_L and C_{Mx} corresponding to Apex 4 or 6 (hereafter called "maximum Apex"). On the other hand, for the wind direction $\theta = 0^o$, the stress ratio does not necessarily becomes the maximum for the combination of C_L and C_{My} corresponding to the Apex 3 or 4. Similar feature is also observed for F2 model. Such cases are summarized in Table 3. In the table, the load combination (i.e. the maximum Apex number) that provides the maximum stress in the member is shown, together with the ratio of the maximum stress to that corresponding to the expected Apex 3 or 4. The ratios for 'Mem' and B3 of F1 model are approximately 1.4, while the ratios range from 1.0 to 1.2 for the other members. The reason why the load combination other than the Apex 3 or 4 induces the maximum stress in the member is not clear at present. However, this may be due to the difference in stress distribution in the roof structure between rigid and flexible roofs. These results suggest that the design wind force coefficients proposed before will be improved so that they can be applied to flexible roofs.

6 EFFECT OF ROOF DEFORMATION

6.1 *CFD analyses of wind forces for the initial roof shapes*

First, CFD analysis is performed for the initial roof shapes of the F1, F2 and S1 models (hereafter "CFD1"). A three dimensional analysis with RANS (Reynolds Averaged Navier-Stokes) model is made by using an open source software named 'OpenFOAM version 1.5' in

Table 4. Boundary condition

Surface at X_{min} (Inlet)	Wind speed: $U_Z = U_{ref} \times (Z/Z_{ref})^{\alpha}$ U_{ref} = 8 m/s; Z_{ref} = 0.6 m; α = 0.18 Turbulence intensity: Experiment values (See Table 5.)
Surface at X_{min} (Outlet)	Surface pressure at outlet: 0 Pa
Surface at X_{min}, Y_{max}, Z_{max}	Free-slip wall
Surface at Z_{min}	No-slip wall
HP surface	No-slip wall

Table 5. Turbulence intensity at inlet

Z (m)	I_u
0 ~ 0.01	0.186
~ 0.02	0.179
~ 0.03	0.186
~ 0.05	0.172
~ 0.10	0.158
~ 0.20	0.111
~ 0.30	0.087
~ 0.40	0.063
~ 0.50	0.047
~ 1.00	0.035

order to calculate the mean C_D, C_L and C_{My} (or C_{Mx}) values. The computational domain is 1.0 × 1.4 × 3.0 m, in which an HP-shaped roof with the same configuration that we used in the wind tunnel experiment is placed as shown in Figure 10. The computation is based on a finite volume method, in which the SIMPLE (Semi-Implicit Method for Pressure Linked Equations) algorithm and the RNG (Re-Normalization Group) k-ε model are used. The boundary condition is summarized in Table 4. The turbulence intensity obtained from the wind tunnel experiment is used (Table 5). The distributions of the wind force coefficients obtained from CFD1 for θ = 0° are shown in Figure 11. Figure 12 shows a comparison for the mean C_L and C_{My} values between experiment and CFD1, and the mean C_D value from CFD1. The values for the S1 model are corrected for the difference in the roof area. It is seen that the results of CFD1 capture the general trend of the experimental results.

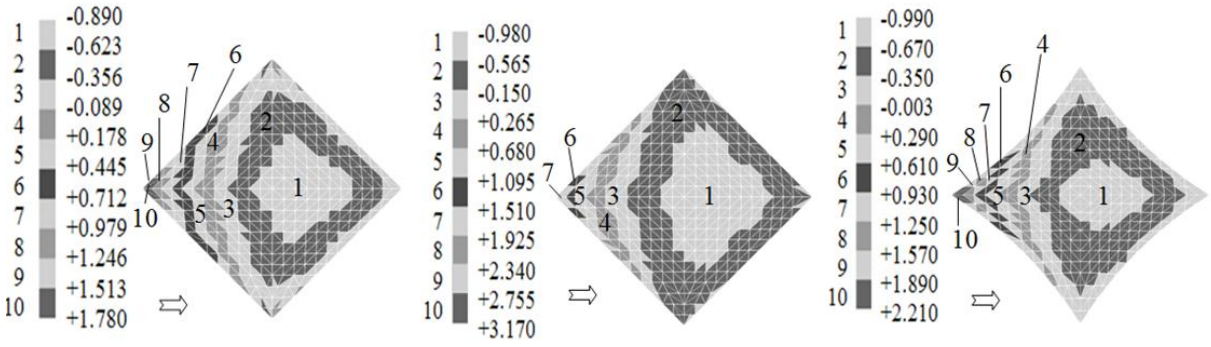

(a) F1 model (θ = 0°) (b) F2 model (θ = 0°) (c) S1 model (θ = 0°)

Figure 11. Wind force coefficients obtained from CFD1 for the initial roof shape

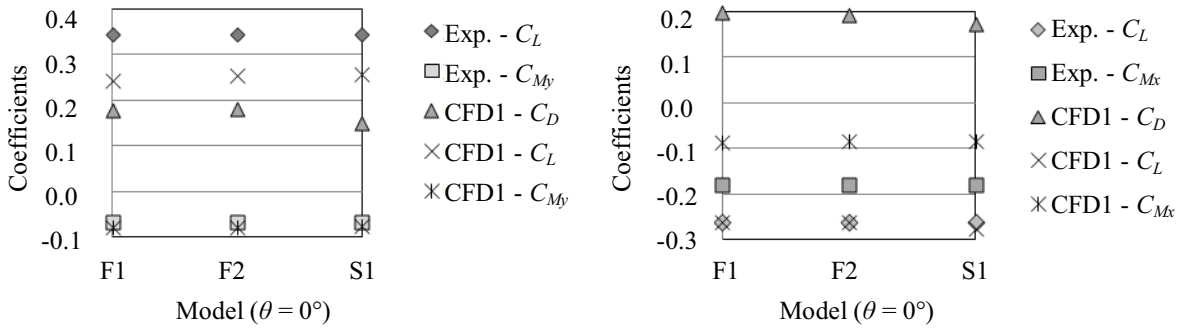

Figure 12. Comparison between experiment and CFD1 for the mean aerodynamic coefficients

6.2 *Effect of roof deformation on the wind forces*

The structural analysis is performed with the mean wind force coefficients obtained from CFD1 (hereafter "SA1"). The design wind speed is 31.5 m/s in the same way as Section 5.2. However, the value of G_f = 1.0 is used to obtain the time-averaged deformation. Then, CFD analysis is again performed for the deformed roofs obtained from SA1 (hereafter "CFD2"). The cross-sections of the roofs are shown in Figure 13. Figure 14 shows the distributions of the mean wind force coefficients on the deformed roofs. Comparing the results with those in Figure 11, it can be seen that the region of upward wind forces expands in the leeward division for the F2 and S1 models. This indicates that the roof deformation in the upward direction causes an increase in the wind force on the roof. Figure 15 shows a comparison for the mean C_D, C_L, and C_{My} values between CFD1 and CFD2. In the figure, the C_L and C_{My} values obtained from CFD2 for F2 and S1 models are approximately 4% to 18% larger than those from CFD1. These features may be caused by the expansion of the upward wind force region that is accompanied by the change of curvature of the membrane surface. Similar feature is observed for the wind direction θ = 90°.

The structural analysis is again made with the mean wind force coefficients obtained from CFD2 (hereafter "SA2"). Figure 16 shows the ratio of the maximum stress obtained from SA2 to that from SA1 for θ = 0°. It is seen that the stresses obtained from SA2 are generally larger than those from SA1. The ratios for the F1 model are up to 1.08, while those for the F2 and S1 models are up to 1.13. Similar feature is also observed for the wind direction θ = 90°. This feature may be related to the increase in the lift coefficient C_L, as shown in Figure 15. Moreover, the feature may be related to the arrangement and stiffness of the elements. From these results, a correction factor for the effect of roof deformation should be introduced in the proposed wind force coefficients.

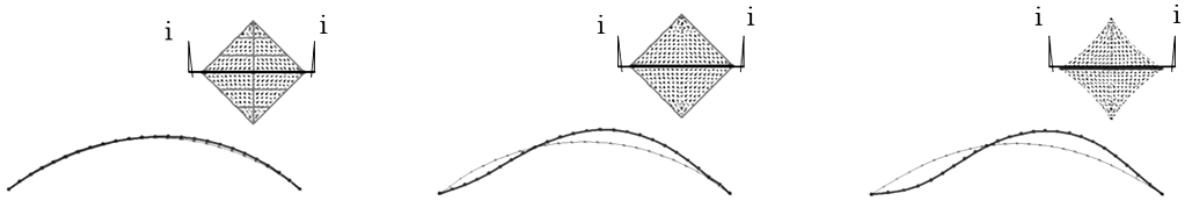

(a) F1 model (b) F2 model (c) S1 model

Scale factor for the displacement: 5 times

Figure 13. Cross-sections (i - i) of the deformed roofs obtained from SA1 for the wind direction θ = 0°

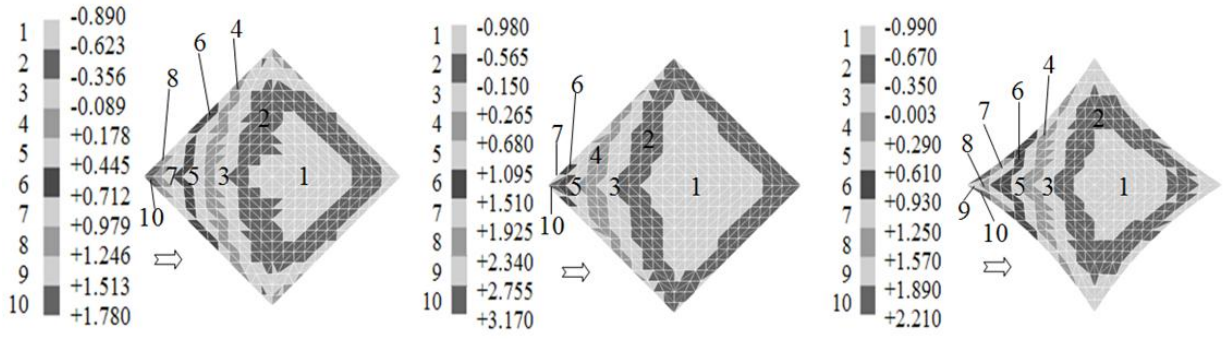

(a) F1 model (θ = 0°) (b) F2 model (θ = 0°) (c) S1 model (θ = 0°)

Figure 14. Wind force coefficients obtained from CFD2 for the deformed shape

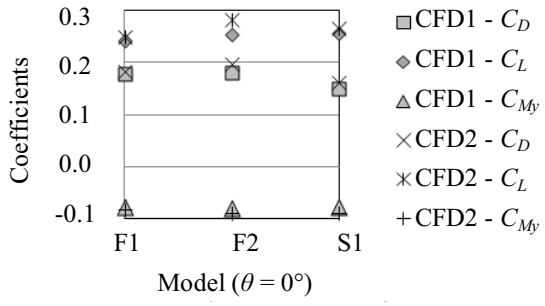

Figure 15. Comparison between CFD1 and CFD2

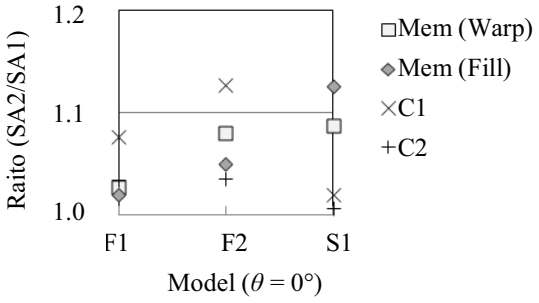

Figure 16. Ratio of the maximum stress obtained from SA2 to that from SA1

7 CONCLUDING REMARKS

The application of the design wind force coefficients obtained from the wind tunnel experiments with rigid models of HP-shaped free roofs to membrane structures has been investigated numerically, based on structural and CFD analyses. Focus is on the supporting system and roof deformation. Three types of membrane structure are considered, i.e. two frame types and one suspension type. First, the structural analyses are performed with the previously proposed design wind force coefficients to investigate the effects of supporting systems on the load effects. The maximum stress ratios for the members are calculated to identify the critical condition providing the maximum load effects. The results suggest that the previously proposed design wind force coefficients should be improved so that they can be applied to membrane roofs. Then, the mean wind forces coefficients on the initial HP-shaped roofs are computed numerically. The structural analysis is made with the mean wind force coefficients obtained from the CFD analysis to predict the time-averaged deformation of the membrane roofs. The CFD analysis on the deformed roofs is performed again. Moreover, the structural analysis is made again with the computed mean wind force coefficients on the deformed roofs. Finally, the load effects obtained from the second structural analyses are compared with those of the first structural analyses. The results indicate that a correction factor for the effect of roof deformation should be introduced in the wind force coefficients.

8 REFERENCES

1 P.K.F. Pun and C.W. Letchford, Analysis of a tension membrane hypar roof subjected to fluctuating wind loads, Third Asia-Pacific Symposium on Wind Engineering, Hong Kong, December 13-15, 1993.
2 Nagai Y., Okada A., Kanda M., Miyasato N. and Saitoh M., Study on wind response on horn-shaped membrane structure, Journal of Structural and Construction Engineering, AIJ, 2012, Vol.77 No.672, pp. 211-219.
3 Uematsu Y., Iizumi, E. and Stachopoulos, T., Wind force coefficients for designing free standing canopy roofs, Journal of Wind Engineering and Industrial Aerodynamics, 2007, Vol.95, pp.1486-1510.
4 Takeda F., Yoshino T. and Uematsu Y., Wind force coefficients for the design of a hyperbolic paraboloid free roof, Proceeding of the International Association for Shell and Spatial Structures (IASS) Symposium, Shanghai, China, 2010.
5 Uematsu Y., Arakatsu F., Matsumoto S. and Takeda F., Wind force coefficients for the design of a hyperbolic paraboloid free roof, Proceeding of Seventh Asia-Pacific Conference on Wind Engineering (APCWE-VII), Taipei, Taiwan, 2009.
6 Takeda F., Yoshino T. and Uematsu Y., Wind force coefficients for the design of a hyperbolic paraboloid free roof, USB flash drive of the 13th International Conference on Wind Engineering, Amsterdam, The Netherlans, 2011.